THE APPLICATION OF THE GURSON-TVERGAARD MODEL IN THE AGING EMBRITTLEMENT OF AUSTENO-FERRITIC STAINLESS STEELS

J.M. Alegre[1], J. Pérez[2], F. Gutiérrez-Solana[2], L. Sánchez[2].

[1] Area de Mecánica de Medios Continuos y T.E.
E. Politécnica Superior de Burgos. Universidad de Burgos
Avda. General Vigón s/n, 09006. Burgos, SPAIN.

[2] Laboratorio de Ciencia e Ingeniería de los Materiales
E.T.S. de Ingenieros de Caminos Canales y Puertos. Universidad de Cantabria.
Avda. Los Castros s/n, 39005. Santander, SPAIN

ABSTRACT

This paper describes the application of the Gurson-Tvergaard model for predicting the elasto-plastic behaviour and the fracture of duplex stainless steels at various levels of aging at 400ºC. In the case of the unaged material, the nucleation of microvoids takes place in Ti carbides formed at the austenitic phase. However, as the material ages, the ferrite becomes steadily harder and breaks through cleavage at decreasing levels of plastic strain. These changes in the fracture micromechanisms can be simulated by means of a variation in the parameters which govern the constitutive equation of the Gurson-Tvergaard model. The simulation performed shows the evolution with time of the embrittlement of these parameters of the Gurson model. The fixing of these parameters has been obtained by comparing the numerical results with those obtained through tensile tests carried out on axisymmetrical notched specimens.

The results obtained confirm that the Gurson-Tvergaard model can be applied in steels in which aging causes changes in their mechanical properties and in their fracture micromechanisms.

INTRODUCTION

The main drawback of duplex steels is the phenomenon of thermal aging, both at high (475ºC) and at low (250-400ºC) temperatures, which drastically reduces their toughness. It has been sufficiently proven that it is the hardening of the ferrite phase with aging which is the cause of the reduction in the overall toughness of the steel [1].

The present paper uses the constitutive Gurson-Tvergaard model [2-4] to simulate the behaviour of a duplex steel with 22% of ferrite phase (22F), unaged and aged for 10000 hours at 400ºC, in order to observe the embrittlement effect on the constitutive parameters of the numerical model.

A methodology will be developed for adjusting the parameters of the Gurson-Tvergaard model using the simulation of notched tensile specimens, and subsequently, the crack growth will be analysed in CT specimens, in order to determine numerically the $J - Da$ curve, and to compare this with the experimental results.

GURSON-TVERGAARD MODEL

The classical porous criterion originally proposed by Gurson [5] and modified by Tvergaard [2,3] is written as follows:

$$\Phi = \frac{3J_2}{s_*^2} + 2f^* q_1 \cosh\left(\frac{q_2 I_1}{2s_*}\right) - (1 + q_1^2 f^{*2}) = 0 \tag{1}$$

where I_1 is the first invariant of stress trace, J_2 is the second invariant of the deviator stress tensor, s_* is the current flow stress and f^*, q_1 and q_2 are the coefficients of the model. Typical values proposed by Tvergaard [2,3] and Needleman [4] for metals are $q_1 = 1.0$ and $q_2 = 1.5$

In order to take into account the effect of the microvoid coalescence as the final stage of the fracture process, Tvergaard [2, 3] introduced the modified porosity value, f^*, as:

$$f^* = \begin{cases} f & \text{si } f < f_C \\ f_C + d(f - f_C) & \text{si } f \geq f_C \end{cases} \tag{2}$$

where f is the volumetric fraction of holes, f_C is the critical porosity at which the interaction between d is the rate of coalescence of the cavities.

The above expressions establish the behaviour of the material in the presence of a specific porosity value. However, as the material is subjected to progressively higher levels of strain, the porosity also increases. There are two phenomena which contribute to the increase in the volumetric fraction of holes. On the one hand, the existing holes gradually grow, making their volumetric fraction increase, and on the other hand, new holes are generated in the material in response to the greater plastic strains [2,3]. Thus, the increase in the porosity will be:

$$df = df_{growth} + df_{nucleation} \tag{3}$$

On the one hand, the increase in the voids is assumed to be proportional to the increase in plastic strain, de^P:

$$df_{growth} = (1-f) \cdot de^P \tag{4}$$

On the other hand, nucleation is a phenomenon which can be controlled by stress, strain, or by a combination of both. Thus the nucleation of new voids is a process requiring substantial experimental support, since it depends heavily on the material under study. One of the most studied cases is that in which the nucleation is controlled by plastic strain and is governed by the following expression:

$$df_{nucleation} = A \cdot de^P \tag{5}$$

where A is the cavity nucleation rate. There are several expressions to define the value of A. In the case of aged duplex stainless steels, several studies [6, 7] have shown that the nucleation is well adjusted for values of $A = cte$.

EXPERIMENTAL PROCEDURE

Material description

The selected steel had a 22% ferrite content and is called 22F. Tables 1 and 2 show the chemical composition and mechanical behaviour at reception conditions.

For this paper, the temperature of 400ºC has been selected for the accelerated aging, as it obtains, in a short test time, a greater variation in the effects on the material: increase in microhardness of the ferrite and overall embrittlement [1].

TABLE 1
CHEMICAL COMPOSITION (% WEIGTH).

Steel	C	Mn	Si	Cr	Ni	Mo
22F	0.045	0.82	1.23	18.4	8.9	2.36

TABLE 2
MECHANICAL PROPERTIES AT RECEPTION CONDITIONS, UNAGED.

Steel	s_y (MPa)	s_u (MPa)	e_u (%)	RA (%)
22F	313	623	41	60

Notched Tensile Specimens Testing

In order to obtain the Gurson-Tvergaard model parameters, tests on axisymmetrical notched specimens (AE) were performed. The specimen geometries are shown in Figure 1. Notched tensile specimens offer the advantage of obtaining a very extensive zone affected solely by nucleation *(A),* which allows this parameter to be well adjusted.
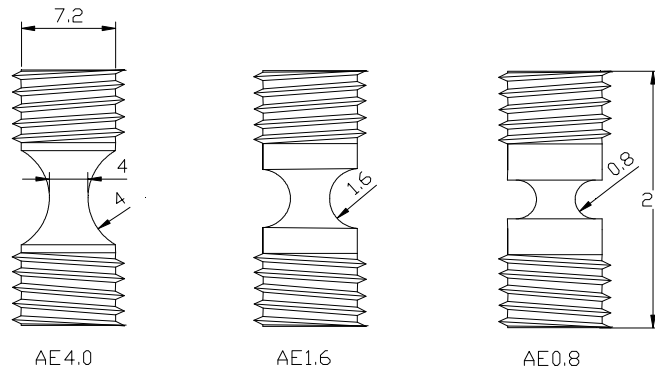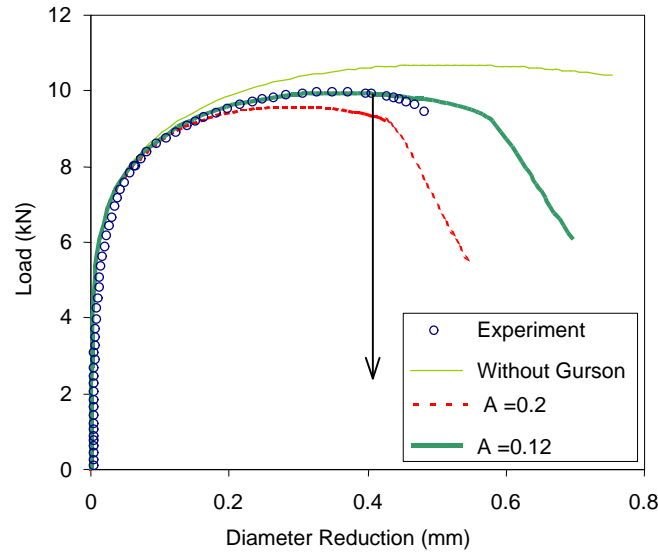

Figure 1: Notched tensile specimens.

The test consists in loading the sample until it fractures and registering the load value and the diametric reduction of the minimum section by means of an extensometer ($P - \Delta f$). Some of the tests were stopped just after the onset of coalescence to allow for metallographical studies of the centre of the neck.

DETERMINATION OF GURSON-TVERGAARD PARAMETERS

The methodology used to determine the Gurson-Tvergaard model parameters, A, f_C, d , is based on a sequential adjustment of the numerical and experimental curves, fixing first the value of the nucleation parameter, A , followed by the critical porosity, f_C and, at the end, the rate of coalescence, d .
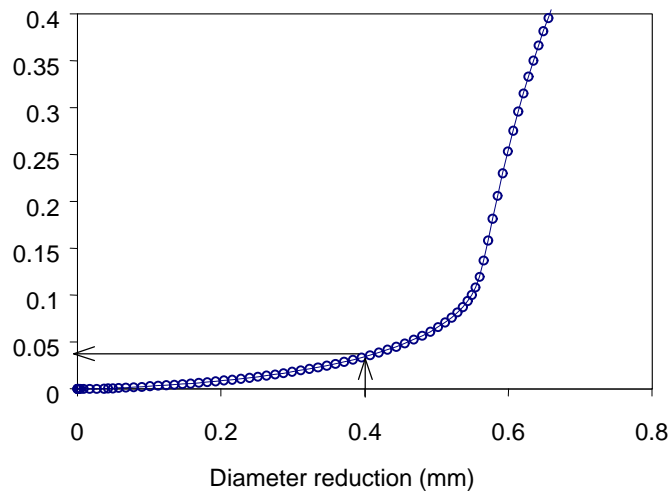
Figure 2 shows the effect of nucleation on the curve $P - \Delta f$ without taking into account the effect of the coalescence, assuming for this $d = 1$, in the behaviour of the aged AE08 specimen. As can be observed, it is easy to determine the nucleation value with the best adjustment, since in this geometry, the fracture does not take place until the final instant of the test. Once the *A* parameter has adjusted the specimen hardening capacity (*A=0.12*), the resistance of the material is overestimated when failing to consider the coalescence of the microvoids.

Figure 2: Influence of void nucleation rate, A, on the curve $P - \Delta f$ of sample AE08. Aged 22F steel.

Thus, the second step consists in determining the value of the porosity starting from which the interaction between the cavities begins, and the subsequent loss of resistant capacity as a result of coalescence. This parameter that is the critical porosity f_C, can be determined through the study of the evolution of porosity in the minimum cross-section during the test.
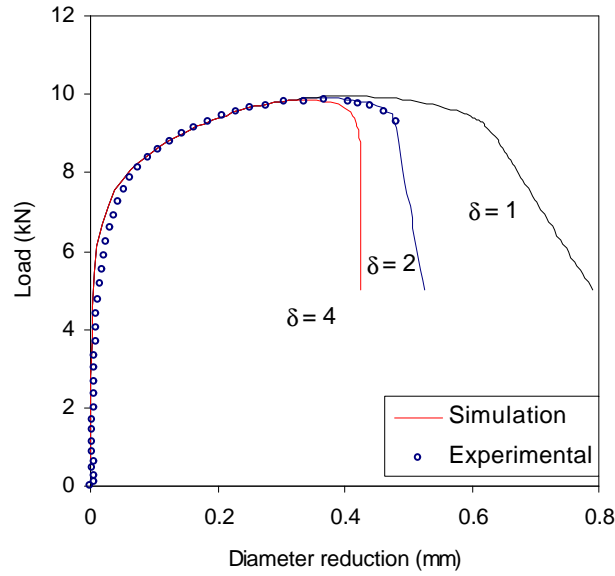
Figure 3 shows the evolution of porosity in the centre of the minimum cross-section, the zone in which fracture is initiated, with respect to the diametric reduction, for the same specimen as in Figure 2, with the nucleation rate $A = 0.12$. It can be observed, following Figures 2 and 3, that the point of separation between the theoretical and the experimental curves is produced for a diametric reduction of $\mathbf{Df} \approx 0.4\ mm$, at which the porosity at the centre has a value of $f_C = 0.04$.

Figure 3: Evolution of porosity in the centre of the minimum cross-section, with respect to the diametric reduction, for $A=0.12$.

The final parameter to adjust refers to the speed with which the coalescence process takes place once the f_C value is surpassed. This parameter, the rate of coalescence $\boldsymbol{d}$, indicates whether the fracture through coalescence in the element occurs rapidly and with little straining capacity (high $\boldsymbol{d}$), or slowly (low $\boldsymbol{d}$).

Figure 4 shows the simulation of the above-mentioned specimen, with a nucleation rate of $A=0.12$, a critical porosity of $f_C = 0.04$ and different values of the rate of coalescence, $\boldsymbol{d}$, together with the experimental curve of the steel aged 10000 hours at 400ºC.

Figure 4: Influence of the rate of coalescence, d, in the AE08 specimen, for $A = 0.12$ and $f_C = 0.04$).

The process of parameter adjustment must be carried out in the three configurations (AE08, AE16 y AE40), to determine the effect of the stress triaxiality on these parameters. Subsequently, the results will be extrapolated for higher triaxialities, with which the parameters required to represent the situation existing at a crack tip, able to model cracked components and specimens, will be obtained.

Thus, for the CT specimen, the P-COD test is modelled and the crack-growth is determined by means of the number of broken elements, starting from the integration points which reach the porosity value $f^* = 1/q_1$, the moment at which, according to equation (1), the material loses all its capacity of resistance.

As the final objective of the simulation of the compact CT specimens is to determine the $J - \Delta a$ curve to compare it with the experimental results, the procedure based on the ESIS standard PI-92 [8] has been used. In this procedure the value of the integral J is obtained as a function of the energy below the P-COD curve and the crack-growth at each instant, $\Delta a = a - a_0$.
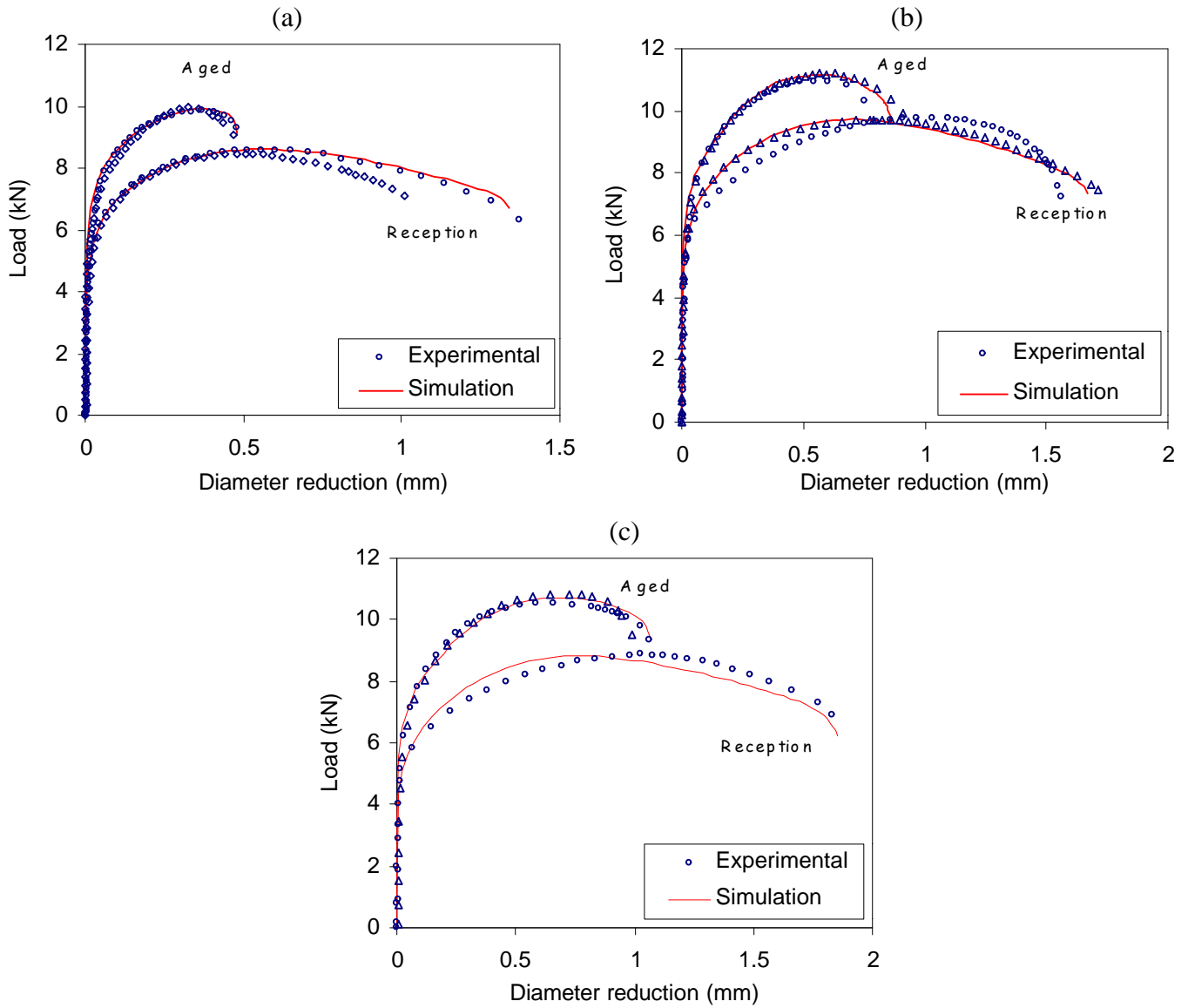

RESULTS AND ANALYSIS

Calculation of the model parameters

Following the methodology presented in the previous section, the adjustment of the $P - \Delta f$ curves has been carried out for the three configurations of the notched tensile specimens shown in Figure 1 (AE08, AE16 y AE40), both for the as-received state steel (unaged) and for the steel aged 10000 hours at 400ºC. The results obtained are shown in Figure 5.

In the unaged steel, it has been verified that a good adjustment is obtained for the three configurations with the same parameters ($A = 0.005$, $f_C = 0.02$, $d = 2.5$), as can be observed in Figure 5. This indicates an independence of the model parameters from the stress triaxiality, or, if there is some dependence, the low value of the nucleation rate, A prevents it from being observed.

However, for the aged steel, the simulation results for the notched tensile samples show a dependence of the nucleation rate, A, on the stress triaxiality, as it can be seen in Table 3, which shows the values of the parameters obtained in the numerical simulation as well as the triaxiality of each type of sample used.

Figure 5: Experimental and numerical curves. (a) AE08, (b) AE16, (c) AE40.

TABLE 3
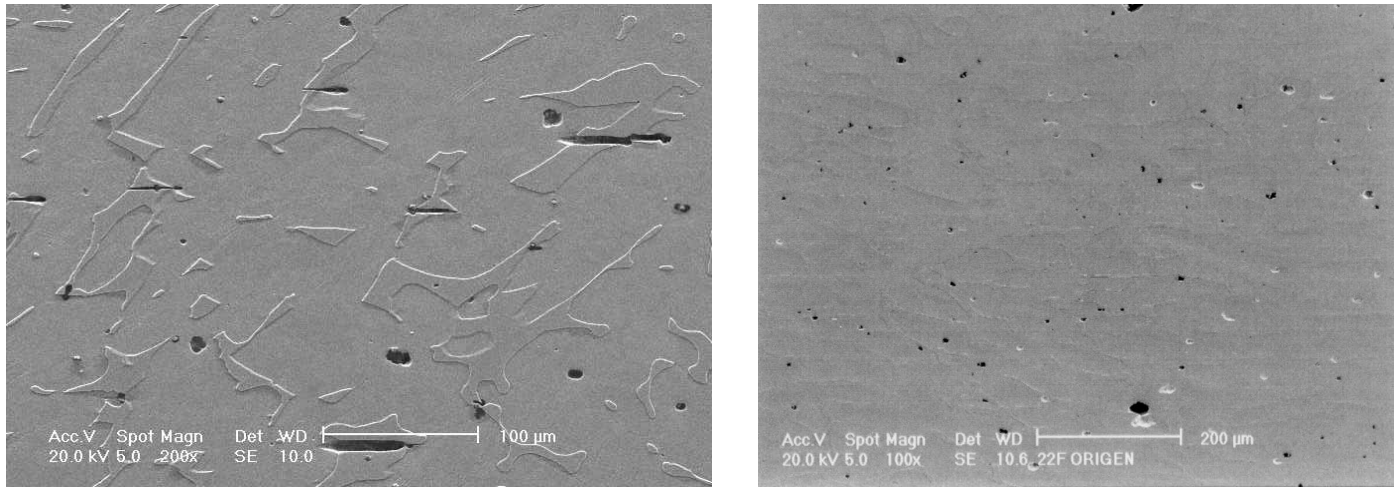FIT PARAMETERS OF THE 22F STEEL AGED FOR 10000 HOURS AT 400ºC.

Configuration	*A*	f_C	*d*	*Triaxiality*
AE08	0.12	0.04	2.0	1.20
AE16	0.10	0.04	2.0	0.81
AE40	0.06	0.04	2.0	0.55

From the representation of the evolution of the nucleation rate with respect to triaxiality for the aged steel, and considering that in the pure compression tests, (triaxiality = -0.33), there are no fractures through formation of microvoids or cleavages, which means a null nucleation rate, it can be estimated that for higher triaxiality values, as is the case of CT samples, the nucleation rate, *A*, tends to a saturation.

The effect of the stress triaxiality on the nucleation rate for the aged steel has its origins in the fracture micromechanisms. When the steel is aged, porosity begins in the form of cleavages in the ferrite as can be observed in Figure 6. The formation of a cleavage occurs as a consequence of a high triaxial state, which explains the fact that the greater the triaxiality, the greater the nucleation.

Another important aspect which can be observed in the metallography of Figure 6 is that the cleavage cracks do not appear simultaneously, but rather do so progressively as the strain increases, as demonstrated by the

difference in the separation between the facets of the cleavage of some cracks compared to others. This fact justifies the use of a nucleation rate, through which the porosity produced by cleavages has been simulated in a gradually increasing way throughout the strain, and not its simultaneous appearance for a critical value of stress or strain.

Figure 6: Metallography of the steel in the aged (left) and unaged states (right). Test interrupted before coalescence.

Figure 6 also shows a metallography of the 22F steel as-received (unaged), underlining the absence of cleavage cracks. The metallographic analysis reveals the presence of Ti carbides inside the holes, mainly occurring at the austenitic phase. Another fact which can be observed in Figure 6 is the low level of porosity reached in the moments prior to fracture, which explains the low value of the nucleation rate, A, obtained for the steel as-received (A=0.005).
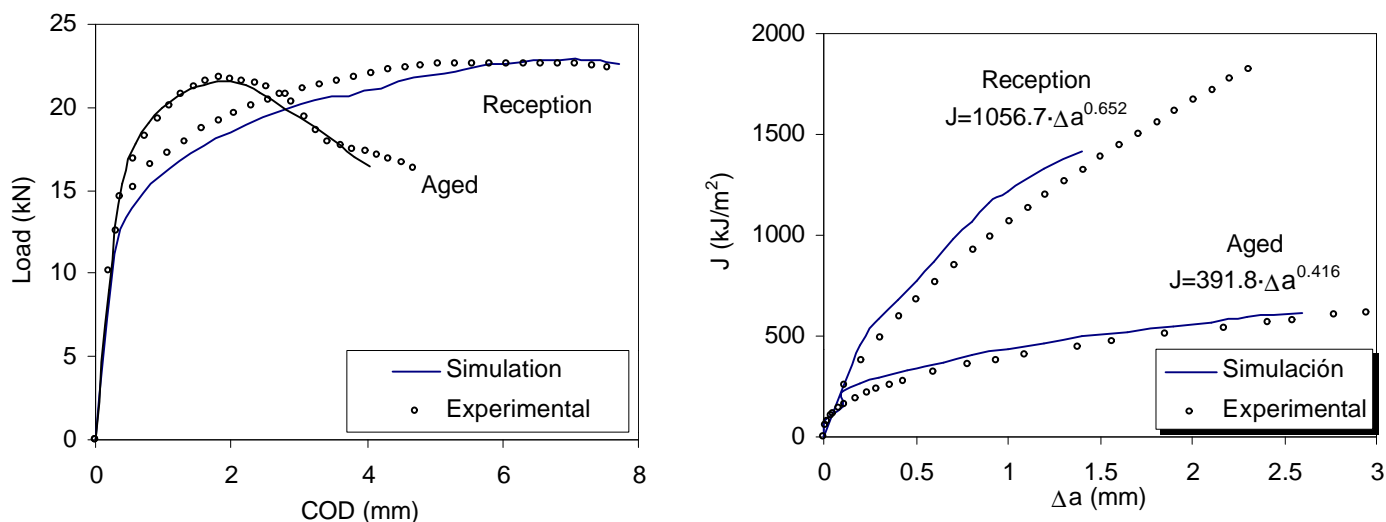
Simulation of fracture behaviour.

Following the methodology presented in the above section, parameters have been determined for the simulation of the compact specimen CT, for the as-received state steel and the steel aged 10000 hours at 400ºC. The values used are shown in Table 4. They have been chosen considering the saturation effect of triaxiality on the aged material.

TABLE 4
GURSON-TVERGAARD MODEL PARAMETERS USED IN THE SIMULATION OF THE CT SPECIMENS.

22F steel	A	f_C	d
Unaged	0.005	0.02	2.5
10000 hours at 400ºC	0.12	0.04	2.0

Figure 7 shows the numerical and experimental *P-COD* curves for the two cases analysed, the as-received and the aged material. The *P-COD* curve and the crack length at each instant are calculated, using the number of elements broken at each step. Then, the $J - Da$ curves are determined. Figure 7 shows also the J_R numerical results obtained for the aged and the as-received steels. The adjustment curve presented in the graph corresponds to several experimental tests carried out by Sanchez [1]. Both types of curves show the good accuracy of the model established to determine the fracture resistance of these duplex stainless steels under the effect of aging embrittlement mechanisms.

Figure 7: Numerical and experimental *P-COD* and $J - Da$ curves for the unaged and aged 22F steel.

CONCLUSIONS

A simulation has been carried out of the elasto-plastic behaviour of an austeno-ferritic steel with a ferrite content of 22%, through the application of the Gurson-Tvergaard model. The results obtained show a good agreement with the experimental results, which indicates that the model can be used for dual-phase steels in which the brittle phase leads to an increase in porosity.

In the unaged steel, the nucleation rate obtained is small, and shows to be independent from the stress triaxiality. However, in the steel aged for 10000 hours at 400ºC, the nucleation rate is around 20 times higher due to the fracture by cleavage of the ferrite, and its value depends on the stress triaxiality.

In the simulation of the CT specimens, the *J-Da* curves have been determined numerically, and good results have been obtained using the Gurson-Tvergaard model parameters corresponding to the highly notched specimen (AE08), in which a triaxiality value is given which is sufficiently representative of that reached at the crack tip.

ACKNOWLEDGEMENTS

REFERENCES

1. Sanchez L. *Ph. Thesis.* 1996. University of Cantabria (Spain).
2. Tvergaard V., *Int. J. Fract.* **17** (1981) 389-407.
3. Tvergaard V., *Int. J. Fract.* **18** (1982) 237-252.
4. Tvergaard V. And Needleman A., *Acta Metall.* **32** (1984) 157-169.
5. Gurson A. L. *Journal of Engineering Materials & Tecnology* **99** (1977) 2-15.
6. Joly P., Pineau A. *Scandinavian Journal of Metallurgy*, **24** (1995) 226-236.
7. Devillers-Guerville L. *Ph Thesis*. École National Supérieure des Mines de Paris. 1998.
8. ESIS P1-92, *European Structural Integrity Society*, Jan 1992.b